Am J Physiol Renal Physiol 321: F480–F493, 2021.
First published August 23, 2021; doi:10.1152/ajprenal.00199.2021

american physiological society

AMERICAN JOURNAL OF PHYSIOLOGY
RENAL PHYSIOLOGY

RESEARCH ARTICLE

Experimental nephrotic syndrome leads to proteolytic activation of the epithelial Na^+ channel in the mouse kidney

Bernhard N. Bohnert,[1,2,3] Daniel Essigke,[1] Andrea Janessa,[1] Jonas C. Schneider,[1] Matthias Wörn,[1] M. Zaher Kalo,[1] Mengyun Xiao,[1] Lingsi Kong,[1] Kingsley Omage,[1] Jörg Hennenlotter,[4] Bastian Amend,[4] Andreas L. Birkenfeld,[1,2,3] and Ferruh Artunc[1,2,3]

[1]*Division of Endocrinology, Diabetology and Nephrology, Department of Internal Medicine, University Hospital Tübingen, Tübingen, Germany;* [2]*Institute of Diabetes Research and Metabolic Diseases, Helmholtz Center Munich, University Tübingen, Tübingen, Germany;* [3]*German Center for Diabetes Research, University Tübingen, Tübingen, Germany; and* [4]*Department of Urology, University Hospital Tübingen, Tübingen, Germany*

Abstract

Proteolytic activation of the renal epithelial Na^+ channel (ENaC) involves cleavage events in its α- and γ-subunits and is thought to mediate Na^+ retention in nephrotic syndrome (NS). However, the detection of proteolytically processed ENaC in kidney tissue from nephrotic mice has been elusive so far. We used a refined Western blot technique to reliably discriminate full-length α-ENaC and γ-ENaC and their cleavage products after proteolysis at their proximal and distal cleavage sites (designated from the NH_2-terminus), respectively. Proteolytic ENaC activation was investigated in kidneys from mice with experimental NS induced by doxorubicin or inducible podocin deficiency with or without treatment with the serine protease inhibitor aprotinin. Nephrotic mice developed Na^+ retention and increased expression of fragments of α-ENaC and γ-ENaC cleaved at both the proximal cleavage site and, more prominently, the distal cleavage site, respectively. Treatment with aprotinin but not with the mineralocorticoid receptor antagonist canrenoate prevented Na^+ retention and upregulation of the cleavage products in nephrotic mice. Increased expression of cleavage products of α-ENaC and γ-ENaC was similarly found in healthy mice treated with a low-salt diet, sensitive to mineralocorticoid receptor blockade. In human nephrectomy specimens, γ-ENaC was found in the full-length form and predominantly cleaved at its distal cleavage site. In conclusion, murine experimental NS leads to aprotinin-sensitive proteolytic activation of ENaC at both proximal and, more prominently, distal cleavage sites of its α- and γ-subunit, most likely by urinary serine protease activity or proteasuria.

NEW & NOTEWORTHY This study demonstrates that murine experimental nephrotic syndrome leads to aprotinin-sensitive proteolytic activation of the epithelial Na^+ channel at both the α- and γ-subunit, most likely by urinary serine protease activity or proteasuria.

epithelial Na^+ channel; nephrotic syndrome; proteolysis; serine proteases

INTRODUCTION

The epithelial Na^+ channel (ENaC) is expressed in the distal nephron and plays a decisive role in the regulation of body Na^+ homeostasis. A specific feature of ENaC is its complex posttranslational processing by proteolysis leading to removal of inhibitory peptide tracts and changes in channel gating (1, 2). ENaC is composed of three subunits (α, β, and γ), and proteolytic cleavage takes place at proximal and distal cleavage sites (designated from the NH_2 terminus; Fig. 1, *A* and *C*) within the extracellular domains of the α- and γ-subunit. Furin, an intracellular serine protease found in the Golgi apparatus, is thought to cleave α-ENaC at the proximal and distal cleavage site, whereas the γ-subunit is only cleaved once at the proximal cleavage site during intracellular maturation (3, 4). A second extracellular cleavage event in distal γ-ENaC leads to the full activation of the channel and is mediated by membrane-bound or extracellular serine proteases such as prostasin (5, 6) or tissue kallikrein (7). Whereas uncleaved ENaC has a low open probability, the removal of the inhibitory tracts from α-ENaC and γ-ENaC increases the open probability to a state of maximal channel activation (8). Using mutants of α-ENaC and γ-ENaC subunits, proteolytic activation of γ-ENaC was found to have a dominant effect on channel activity, stimulating channel activation in the absence of proteolysis of α-ENaC (9).

Proteolytic activation of ENaC by aberrantly filtrated serine proteases or proteasuria is thought to occur during nephrotic syndrome, thereby causing Na^+ retention and

Correspondence: F. Artunc (ferruh.artunc@med.uni-tuebingen.de).
Submitted 19 May 2021 / Revised 23 July 2021 / Accepted 17 August 2021

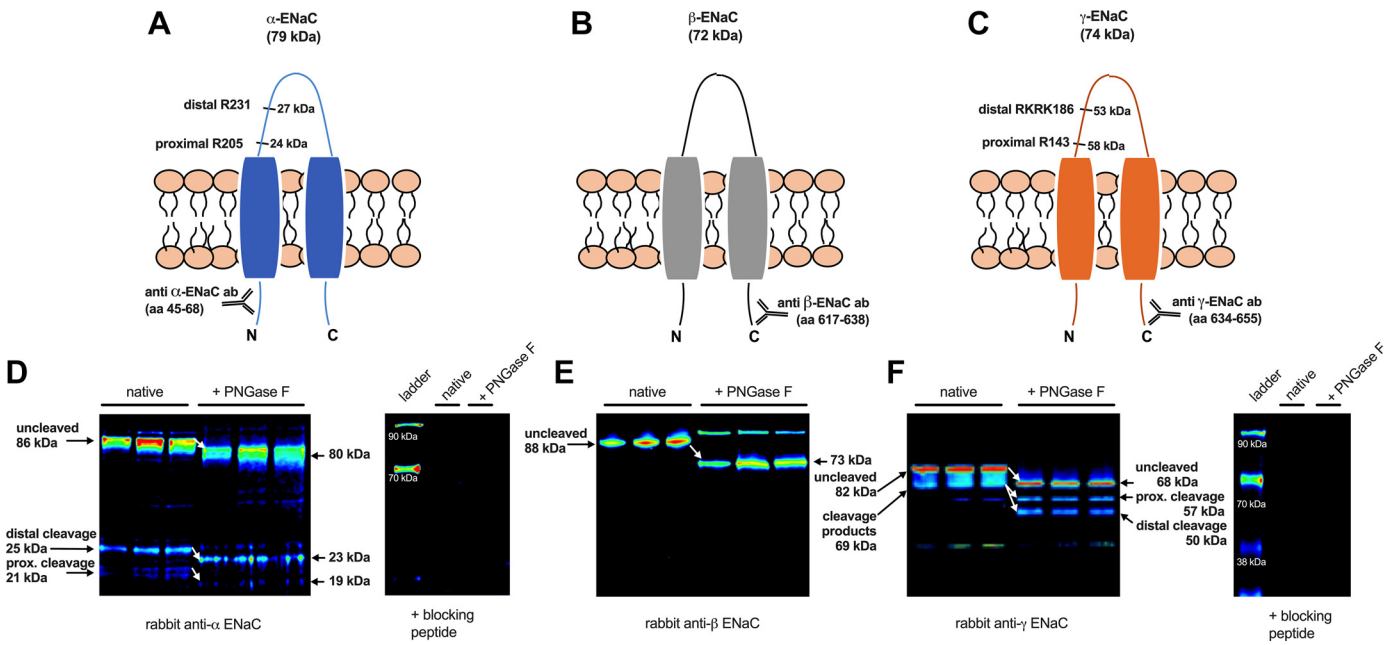

Figure 1. Expression of epithelial Na^+ channel (ENaC) subunits in the kidney cortex of healthy wild-type mice and the effect of deglycosylation. *A–C*: localization of the immunogenic sequences of the used antibodies against murine α-ENaC, β-ENaC, and γ-ENaC. In α-ENaC and γ-ENaC, the proximal and distal cleavage sites (designated from the NH_2-terminus, respectively) are depicted. The antibody against NH_2-terminal α-ENaC is supposed to detect full-length α-ENaC at 79 kDa (699 amino acids) and two NH_2-terminal fragments with a mass of 27 kDa (231 amino acids) and 24 kDa (205 amino acids). The antibody against COOH-terminal β-ENaC is supposed to detect full-length β-ENaC at 72 kDa (638 amino acids). The antibody against COOH-terminal γ-ENaC is supposed to detect full-length γ-ENaC at 74 kDa (655 amino acids) and COOH-terminal fragments with a mass of 58 kDa (512 amino acids) after proximal cleavage and at 53 kDa (469 amino acids) after distal cleavage, respectively. Mass values were calculated from the amino acid sequences (omitting any *N*-glycosylations). *D–F*: Western blots of kidney lysates for the expression of ENaC subunits. Deglycosylation of the samples with peptide:*N*-glycosidase F (PNGase F) induces a shift (white arrows) of the migration of the bands by 6 kDa for full-length α-ENaC and 2 kDa for proximally and distally cleaved α-ENaC, by 15 kDa for full-length β-ENaC, and by 14 kDa for full-length γ-ENaC. Moreover, deglycosylation revealed two additional bands for γ-ENaC, representing proximally and distally cleaved γ-ENaC. Administration of the blocking peptide for α-ENaC and γ-ENaC attenuated all bands. Note that deglycosylation negatively impacted on the appearance of the bands representing the cleavage products of α-ENaC, which was due to PNGase F (37 kDa). prox., proximal.

edema (10–14). This concept is supported by our findings that treatment with the serine protease inhibitor aprotinin prevented Na^+ retention in mice with experimental nephrotic syndrome, as did treatment with the ENaC blocker amiloride (13, 15, 16). A limitation of these studies was the failure to demonstrate the expression of cleaved ENaC subunits, particularly that of cleaved γ-ENaC in kidney lysates from nephrotic mice by Western blot analysis. This was in sharp contrast to Western blot analyses of γ-ENaC expressed in oocytes, which, using the same antibody, revealed the expression of fully cleaved γ-ENaC after the addition of chymotrypsin, plasmin, or plasma kallikrein (17, 18).

In rat ENaC, there are 6, 12, and 5 consensus sites (Asn-X-Ser/Thr) for *N*-glycosylation in the extracellular domains of the α-, β-, and γ-subunits, respectively (19), that are required for maturation and surface expression (20). In Madin-Darby canine kidney cells expressing αβγ-ENaC, *N*-glycosylation was found to involve all ENaC subunits (21). This finding was reproduced in rats in 2006 by Ergonul et al. (22). In both studies, ENaC subunits were deglycosylated using the enzyme peptide:*N*-glycosidase F (PNGase F). Recently, Frindt et al. (23) reported the identification of fully cleaved γ-ENaC in kidneys from healthy mice and rats after deglycosylation using PNGase F. In their discussion, they encouraged efforts to translate these findings to rodents with experimental nephrotic syndrome to finally prove the occurrence of proteolytic activation of γ-ENaC in vivo.

In this study, we tested the hypothesis that experimental nephrotic syndrome leads to proteolytic activation of the α-subunit and particularly of the γ-subunit of ENaC in kidneys from nephrotic mice. We demonstrated that nephrotic syndrome led to increased expression of cleavage products of both α-ENaC and γ-ENaC, which was prevented by the serine protease inhibitor aprotinin. Moreover, salt intake or treatment with ENaC blocker triamterene or aldosterone also modulated expression of ENaC cleavage products.

METHODS

Mouse Experiments

Experiments were performed on 3-mo-old wild-type 129S1/SvImJ mice of both sexes at a ratio of 1:1, which are susceptible to the induction of experimental nephrotic syndrome by doxorubicin (24, 25). In addition, mice with inducible podocin deficiency were used as an alternative nephrotic mouse model [B6-Nphs2$^{tm3.1Antc}$*Tg(Nphs1-rtTA*3G)^{8Jhm}*Tg(tetO-cre)^{1Jaw} or *nphs2*$^{\Delta ipod}$] (15). Genotyping was done using PCR as previously described (15). Mice were kept on a 12:12-h light-dark cycle and fed a standard diet (ssniff, Na^+ content: 0.24% corresponding to 104 μmol·g^{-1}, Soest, Germany) with tap water ad libitum.

Experimental nephrotic syndrome was induced in 129S1/SvImJ mice after a single intravenous injection of doxorubicin (14.5 μg·g body wt^{-1}, Medac, Germany) as previously developed by our group (24–26). *Nphs2*$^{\Delta ipod}$ mice were induced by a 14-day treatment with doxycycline in the drinking water (2 g·L^{-1} with 5% sucrose). Treatment with the serine protease inhibitor aprotinin (6,000 KIU·mg^{-1}, Loxo, Heidelberg, Germany) was performed using custom-made subcutaneous pellets with a matrix-driven sustained release (Innovative Research of America). Aprotinin-containing or placebo pellets consisting of the matrix only were surgically implanted subcutaneously on the back of the mice on *day 3* after end of the induction as previously described (26). The optimal dose chosen after dose-finding experiments was 1 mg in doxorubicin-induced nephropathy and 2 mg·day^{-1} in *nphs2*$^{\Delta ipod}$ mice. To block the effects of aldosterone, the mineralocorticoid receptor (MR) antagonist canrenoate (aldactone) was offered in the drinking bottle (400 mg·L^{-1}) starting on *day 3* after doxorubicin injection. Due to restrictions by the regulating authority and the Institutional Animal Care and Use Committee, which would not allow us to study mice in metabolic cages for Na^+ balance over 5 or more days, we kept single mice in normal cages and collected spontaneously voided urine in the morning between 8 and 9 AM. Daily food and fluid intake were monitored by weighing the food pellets and water bottle. Mice were euthanized on *days 4*, *8*, and *14* as designated, and blood and kidneys were collected.

To study the impact of salt intake and certain drugs on proteolytic processing of ENaC in vivo, we treated healthy 129S1/SvImJ mice with a low-salt diet (C1036, Altromin, Lage, Germany, Na^+ content: 7 μmol·g^{-1} food) or with treatment with high salt (0.9% NaCl in tap water), triamterene (200 mg·L^{-1} in drinking water), aldosterone (10 μg·g body wt^{-1} in 1 μL·g^{-1} DMSO ip), dexamethasone (10 μg·g body wt^{-1} in 10 μL saline ip), or canrenoate (400 mg·L^{-1} in drinking water, corresponding to ~80 μg·g body wt^{-1}). Urine was collected in metabolic cages before and during treatment over 2 days, respectively. Mice were euthanized after that, and blood and kidneys were collected. All animal experiments were conducted according to the National Institutes of Health's *Guide for the Care and Use of Laboratory Animals* and the German law for the welfare of animals, and they were approved by local authorities (Regierungspraesidium Tuebingen, Approval Nos. M5/16, M5/17, and M02/19M).

Human Samples

The Department of Urology provided small snap-frozen samples of the human kidney from nephrectomy specimens of patients with renal cell carcinoma. Histological analysis confirmed that samples contained healthy kidney tissue. Before nephrectomy, patients had given informed consent to make the tissue available for research. The asservation of kidney samples was approved by the local ethics committee (379/2010BO2).

Laboratory Measurements

Urinary protease activity was measured using the chromogenic substrate S-2251 (Haemochrom, Essen, Germany), and 3 μL urine and 50 μL of 2 mM substrate were incubated for 1 h at 37°C with or without aprotinin (final concentration: 20 μg·mL^{-1}). Absorption was analyzed at 405 nm on a 96-well plate reader (EL800, Biotek). The difference between the optical density with or without aprotinin reflected the specific activity of serine proteases. Values are expressed as relative units (1,000 × change in absorption at 405 nm) after 1 h of incubation.

Urinary creatinine was measured with a colorimetric Jaffé assay (Labor + Technik, Berlin, Germany), urinary protein concentration was measured using the Bradford method (Bio-Rad Laboratories, Munich, Germany), and urinary Na^+ concentration was measured with flame photometry (EFUX 5057, Eppendorf, Hamburg, Germany). Both urinary protein and Na^+ concentrations from voided urine samples were normalized to the urinary creatinine concentration. Plasma aldosterone was measured using an ELISA kit (IBL, Hamburg, Germany).

Western Blot Analysis of Kidney Tissue of Mice and Humans

Half the kidney per mouse was sliced, and the cortex was dissected using a scalpel. Nephrectomy specimens were used as provided from the Department of Urology. Homogenization was performed using a Dounce homogenizer in 1 mL lysis buffer containing 250 mM sucrose, 10 mM triethanolamine HCl, 1.6 mM ethanolamine, and 0.5 EDTA at pH 7.4 (all Sigma) (27). During all preparation steps, aprotinin (40 μg·mL^{-1}) and a protease inhibitor cocktail (final concentration: 0.1× stock, Mini-complete, Roche) was present to avoid ENaC cleavage in vitro. Homogenates were centrifuged at 1,000 *g* for removal of the nuclei. Subsequently, the supernatant was centrifuged at 20,000 *g* for 30 min at 4°C, and the resulting pellet containing plasma membranes was resuspended and diluted to a concentration of 5 mg·L^{-1}. This yielded higher ENaC signals compared with centrifugation at 300,000 *g*. Samples were deglycosylated using PNGase F according to the manufacturer's instructions (NEB). First, samples were denaturated with glycoprotein denaturing buffer. Samples were then incubated with glycobuffer, Nonidet P-40, and PNGase F for 1 h at 37°C. Native samples without deglycosylation were boiled in Laemmli buffer at 70°C for 10 min. Subsequently, 20 μg of sample were loaded on an 8% (γ-ENaC) or a 4–15% (α- and β-ENaC) polyacrylamide gel for electrophoresis. After transfer to nitrocellulose membranes, the blocked blots were incubated with the primary antibodies against the ENaC subunits overnight at 4°C after 1:1,000 dilution in blocking buffer (Li-Cor). After detection of α-ENaC, membranes were stripped for detection of β-ENaC. ENaC subunits were detected with fluorescent secondary antibody labeled with IRDye 800CW or IRDye 680RD and a fluorescence scanner (Li-Cor Odyssey). As a loading control, total protein was measured using Revert Total Protein Stain (Li-Cor).

Primary Antibodies

Antibodies against murine α-ENaC and β-ENaC were raised in rabbits against the amino acids 45–68 for α-ENaC and 617–638 for β-ENaC using a commercial service (Pineda, Berlin, Germany). Anti-γ-ENaC was purchased from Stressmarq (SPC-405, Victoria, BC, Canada). This antibody had been raised in rabbits against COOH-terminal amino acids

634–655 of γ-ENaC (Fig. 1, *A*, *C*, and *E*). All antibodies were based on the peptide sequences first introduced and validated by Masilamani et al. (28) and used by many other researchers in the field such as in the work of Frindt et al. (23). The antibodies against α-ENaC and β-ENaC had been affinity purified, whereas anti-γ-ENaC had been purified with protein A according to the manufacturer. To confirm that the observed bands were specific for α-ENaC and γ-ENaC, the primary antibody was blocked after preincubation with custom-made immunogenic peptides (20× excess by molarity) overnight at 4°C. In addition, the antibodies were validated using lysates from *Xenopus* oocytes expressing murine αβγ-ENaC against lysates from sham-injected oocytes. Oocyte lysates were kindly provided by Dr. Alexandr Ilyaskin and Prof. Christoph Korbmacher (University of Erlangen, Erlangen, Germany).

Statistical Analysis

Data are provided as means ± SE. Data were tested for normality with a Kolmogorov–Smirnov test, D'Agostino and Pearson omnibus normality test, and Shapiro–Wilk test. Variances were tested using Bartlett's test for equal variances. Accordingly, data were tested for significance with parametric or nonparametric ANOVA followed by Dunnett's, Dunn's, or Tukey's multiple comparison posttests, paired or unpaired Student's *t* tests, or a Mann–Whitney *U* test where applicable using GraphPad Prism 9 (GraphPad Software, San Diego, CA, www.graphpad.com). To analyze more than 18 samples with Western blot, two or more gels were loaded each with two or three samples from all groups to be compared. The signal of the samples of the healthy control group in each gel was averaged and set to 100%. The effect of the treatment on the band density was expressed relative to this value. The reported mass values of the bands are the arithmetic mean of the values obtained from all blots. A P value of <0.05 at two-tailed testing was considered statistically significant. Densitometric analysis of the Western blots was done using Image Studio version 3.1.4 and Empiria Studio version 1.3.0.83 (Li-Cor).

RESULTS

Deglycosylation of Kidney Lysates Leads to a Shift in the Migration of All ENaC Subunits and Reveals the Expression of γ-ENaC Cleavage Products

Western blot analysis from murine kidney cortex samples for α-ENaC revealed three bands at 86, 25, and 21 kDa, all of which disappeared after application of the immunogenic peptide (Fig. 1, *A* and *D*). For β-ENaC, there was only a single band at 88 kDa corresponding to the full-length subunit, which is not proteolytically processed (Fig. 1, *B* and *E*). For γ-ENaC, there was a band at 82 kDa, and below this a blurry signal extended until 69 kDa (Fig. 1, *C* and *F*). Application of the immunogenic peptide blocked these signals.

Deglycosylation of the same samples using PNGase F led to characteristic shifts of the migration pattern of all ENaC subunits. α-ENaC migrated at 80, 23, and 19 kDa, which could also be blocked by application of the immunogenic peptide (Fig. 1*D*). Migration of the band for full-length β-ENaC was shifted by 15 kDa to 73 kDa, and, unexpectedly, there appeared a second band at 102 kDa (Fig. 1*E*). The most significant change was obtained for γ-ENaC. As shown in Fig. 1*F*, the migration pattern changed with three separate bands arising at 68, 57, and 50 kDa, all of which were blocked by application of the immunogenic peptide. The molecular mass of the obtained bands approximated the expected mass of full-length (74 kDa), proximally cleaved (58 kDa), and distally cleaved γ-ENaC (53 kDa; Fig. 1*F*). The obtained difference between full-length and proximally cleaved γ-ENaC was 11 kDa and that between proximally cleaved and fully cleaved γ-ENaC was 7 kDa, which was also in good agreement to the expected values (15 and 5 kDa, respectively). In conclusion, these results using a commercially available rabbit antibody against COOH-terminal γ-ENaC and deglycosylated kidney lysates reproduce the results from the work of Frindt et al. (23).

Experimental Nephrotic Syndrome in Mice Leads to Increased Expression of Proximally and Distally Cleaved α-ENaC and γ-ENaC

The above-mentioned results set the basis to investigate the presence of proteolytic activation of ENaC by cleavage of its α- and γ-subunits in experimental nephrotic syndrome in mice, which has been a missing proof in our previous efforts (13, 15, 16, 18). After the induction of nephrotic syndrome by doxorubicin, mice rapidly developed proteinuria along with proteasuria, urinary Na^+ retention, and body weight gain (Fig. 2, *A–D*). In a previous study (16), renal Na^+ retention, as evidenced from urine collections for 24 h, had been demonstrated in doxorubicin-injected nephrotic mice. The plasma aldosterone concentration was significantly increased in nephrotic mice (Fig. 2*E*). Similar changes were observed in mice with inducible podocin deficiency, as previously described (15). In both models, for unknown reasons, Na^+ retention and body weight gain were spontaneously reversed thereafter, which have been previously described for nephrotic rats (29) and seems to be characteristic for experimental nephrotic syndrome in rodents.

In doxorubicin-injected nephrotic mice, expression of ENaC subunits was analyzed at different timepoints using Western blot analysis. In doxorubicin-injected nephrotic mice, expression of full-length α-ENaC, β-ENaC, and γ-ENaC was not appreciably altered on *day 4* before the nephrotic phase with Na^+ retention and body weight gain and during the nephrotic phase on *day 8*, whereas there was increased expression of full-length β-ENaC and γ-ENaC on *day 14* after the nephrotic phase (Fig. 2, *F* and *H–N*). The cleavage product of α-ENaC at 25 kDa was upregulated at *day 8* and then normalized at *day 14* (Fig. 2*I*). The cleavage product of α-ENaC at 21 kDa was of very low abundance and became slightly visible in nephrotic mice at *day 8* (Fig. 2, *F* and *J*). Expression of the cleavage product of γ-ENaC at 57 kDa and most prominently that at 50 kDa was markedly increased on *days 8* and *14*, reaching statistical significance (Fig. 2, *M* and *N*). On *day 14* after the reversal of Na^+ retention, expression of the γ-ENaC cleavage product at 50 kDa tended to decrease, whereas the cleavage product at 57 kDa was still increased (Fig. 2*N*).

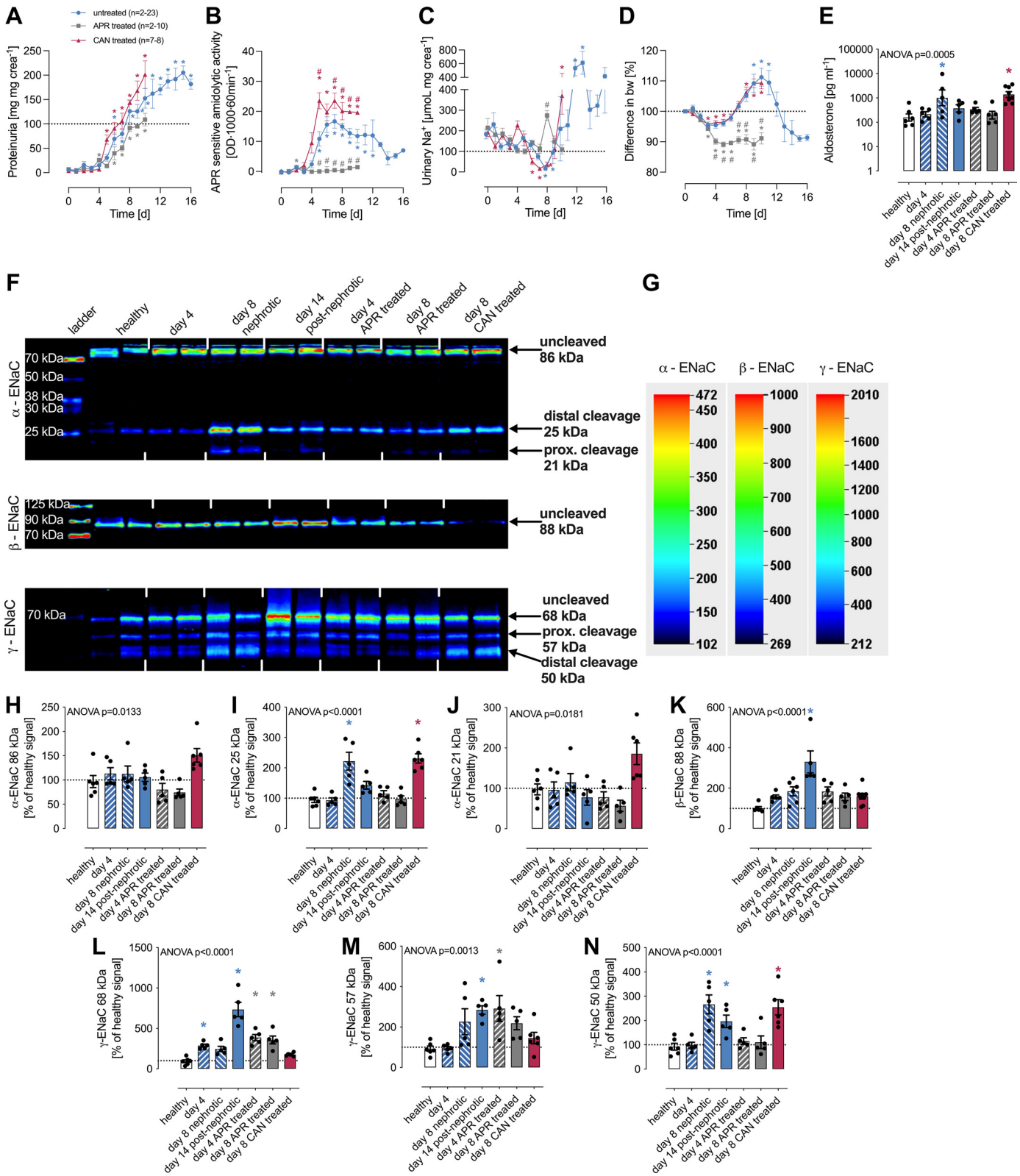

Effect of the Serine Protease Inhibitor Aprotinin and the MR Antagonist Canrenoate on Proteolytic ENaC Activation in Experimental Nephrotic Syndrome

To study the impact of urinary serine protease activity and aldosterone on Na^+ retention and the expression of ENaC subunits in experimental nephrotic syndrome, we treated mice with the serine protease inhibitor aprotinin and the MR antagonist canrenoate, beginning on *day 3* after induction. As shown in Fig. 2, *A–E*, aprotinin did not reduce proteinuria but inhibited urinary serine protease activity and prevented Na^+ retention while reducing hyperaldosteronism. Canrenoate did not have an effect on all of these parameters.

In Western blot analyses of doxorubicin-treated mice, aprotinin had no effect on the expression of the distal cleavage products of α-ENaC and γ-ENaC at 25 and 50 kDa, respectively, on *day 4* (Fig. 2, *F–N*). However, on *day 8*, aprotinin completely inhibited the upregulation of these cleavage products seen in untreated nephrotic mice. In contrast, treatment of nephrotic mice with canrenoate had no effect on the expression of these cleavage products.

To replicate these results in another nephrotic mouse model, we analyzed kidneys from mice with inducible podocin deficiency. As shown in Fig. 3, we could reproduce the increased expression of the distal cleavage products of α-ENaC and γ-ENaC at 25 and 50 kDa, whereas the expression of the other bands was not altered. In aprotinin-treated nephrotic mice, expression of these cleavage products was normalized or even suppressed (Fig. 3).

Proteolytic Activation of ENaC Can Be Stimulated in Healthy Mice in Vivo

To further validate the physiological significance of the obtained cleavage products of α-ENaC and γ-ENaC, we subjected healthy wild-type mice to maneuvers that we thought might also involve proteolytic activation of ENaC. For stimulation, we used low-salt intake, ENaC blockade using triamterene, and administration of aldosterone and dexamethasone. For suppression, we used high-salt intake and the MR antagonist canrenoate. Kidneys were harvested after 48 h of treatments to capture the changes in proteolytic processing that were expected to take place rapidly (30).

The 24-h urinary Na^+ excretion under the various treatments is shown in Fig. 4*A*. The changes of 24-h urinary Na^+ excretion were, if not compensated, paralleled by the changes in body weight (Fig. 4*B*) and mirrored by opposite changes of the plasma aldosterone concentration (Fig. 4*C*).

Figure 4, *D–L*, shows the corresponding Western blot analyses and densitometry from kidney cortex lysates of these mice. Compared with control conditions, treatments had no effect on the expression of full-length α-ENaC and β-ENaC (Fig. 4, *F* and *I*), whereas expression of full-length γ-ENaC tended to be higher in high-salt-treated mice and lower in low-salt- or aldosterone-treated mice (Fig. 4*J*). Treatments also modulated proteolytic processing of α-ENaC and γ-ENaC. Stimulation of ENaC activity, such as with low-salt intake or administration of aldosterone or triamterene, increased the expression of proximally and distally cleaved α-ENaC and γ-ENaC (Fig. 4, *G*, *H*, *K*, and *L*). In contrast, high-salt intake led to reduced expression of cleaved α-ENaC and γ-ENaC. Treatment with dexamethasone or canrenoate had no appreciable effect on the expression of ENaC subunits.

To investigate whether stimulation of proteolytic ENaC processing by low-salt diet involves MR, additional experiments were carried out with simultaneous canrenoate treatment of the mice. As shown in Fig. 5, canreonate treatment inhibited all effects induced by a low-salt diet, such as upregulation of the distal cleavage products of α-ENaC and γ-ENaC at 25 and 50 kDa and suppression of full-length γ-ENaC.

Expression of γ-ENaC in the Kidney Cortex From Human Nephrectomy Specimens

Finally, we aimed to reproduce the results with human kidney samples obtained from nephrectomy specimens (n = 16). These patients (9 men and 7 women) had a median age of 69 yr (interquartile range: 65–75 yr) and normal kidney function [median estimated glomerular filtration rate: 83 $mL \cdot min^{-1} \cdot 1.73\ m^{-2}$ (range: 68–94 $mL \cdot min^{-1} \cdot 1.73\ m^{-2}$)]. According to urine dipstick testing, slight proteinuria (+) was present in six patients, whereas eight patients had evidence of microhematuria. Western blot analysis from these samples for α-ENaC and β-ENaC using the same custom-made antibodies as used for mouse samples as well as antibodies from a commercial vendor did not result in plausible signals. However, for γ-ENaC, there were three bands at 81, 63, and 48 kDa, and deglycosylation using PNGase F shifted the molecular mass to 68, 56, and 45 kDa. Application of the immunogenic peptide blocked all of the observed bands obtained from native and deglycosylated samples (Fig. 6, *A–C*). As in mouse samples, the obtained bands were suggestive of full-length, proximally cleaved, and distally cleaved γ-ENaC, respectively; however, their molecular mass was lower than the expected mass calculated from the amino acid sequence. The difference between full-length and proximally cleaved γ-ENaC was 12 kDa and that between proximally and distally cleaved γ-ENaC was 11 kDa, which was in fair agreement to the expected values (15 and 5 kDa, respectively). The expression was highly variable in this small sample, spanning a factor of 10 (Fig. 6*D*).

Figure 2. Expression of epithelial Na^+ channel (ENaC) subunits in the kidney cortex from doxorubicin-induced nephrotic mice with or without treatment with the serine protease inhibitor aprotinin (APR) or the mineralocorticoid receptor antagonist canrenoate (CAN). *A–D*: course of proteinuria, proteasuria, urinary Na^+ excretion, and body weight (bw). *E*: plasma aldosterone concentration under different timepoints and treatments. *F*: Western blots of expression of α-ENaC, β-ENaC, and γ-ENaC under different timepoints and treatments. Signal intensity is depicted using a color spectrum to achieve the highest resolution between weak and strong bands. Western blot analysis of the expression of α-ENaC and β-ENaC was performed using native samples. Analysis of the expression of γ-ENaC was done using peptide:*N*-glycosidase F (PNGase F)-treated samples. Blots were additionally stained for total protein content. *G*: color bars representing signal intensity. *H–N*: densitometric analysis of the Western blot results from two gels and n = 5 or 6 per group normalized for the total protein signal of each lane. Values are expressed relative to the average of the healthy control group. *Significant difference compared with healthy mice; #significant difference compared with untreated mice. d, days; OD, optical density; prox., proximal.

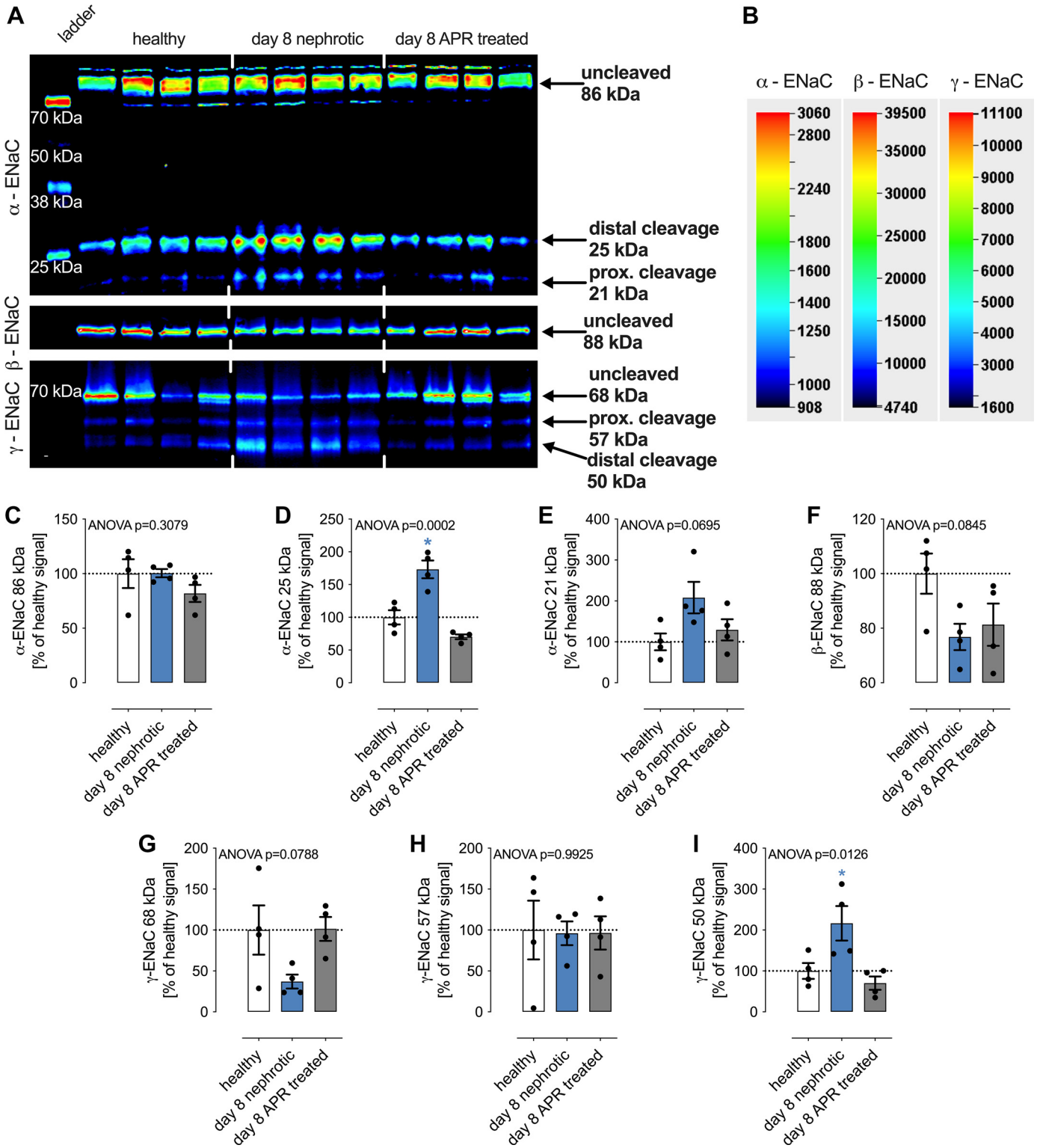

Figure 3. Expression of epithelial Na^+ channel (ENaC) subunits in the kidney cortex from podocin-deficient nephrotic mice with or without treatment with the serine protease inhibitor aprotinin (APR). *A*: expression of α-ENaC, β-ENaC, and γ-ENaC as analyzed by Western blot from plasma membrane proteins. Western blot analysis of the expression of α-ENaC and β-ENaC was performed using native samples. Analysis of the expression of γ-ENaC was done using peptide:*N*-glycosidase F-treated samples. Blots were additionally stained for total protein content. *B*: color bars representing signal intensity. *C–I*: densitometric analysis of the Western blot results ($n = 4$ per group) normalized for the total protein signal of each lane. *Significant difference compared with healthy mice. prox., proximal.

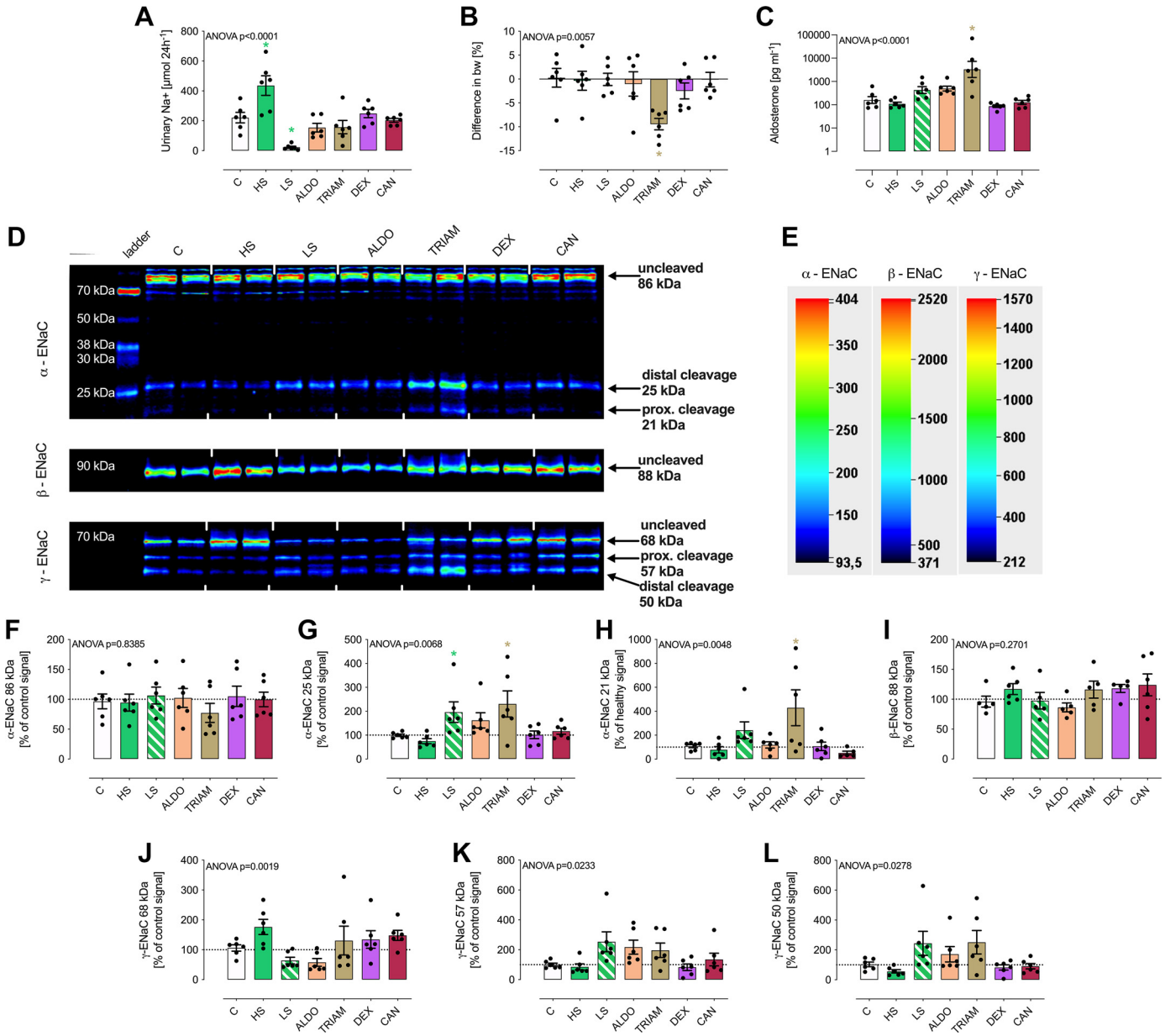

Figure 4. Effect of salt intake or drug treatment on expression of epithelial Na^+ channel (ENaC) subunits in the kidney cortex of mice. *A*–*C*: 24-h urinary Na^+ excretion, body weight (bw) change, and plasma aldosterone concentration under control (C), high-salt (HS) diet, and low-salt (LS) diet, as well as after treatment with aldosterone (ALDO), triamterene (TRIAM), dexamethasone (DEX), and canrenoate (CAN). *D*: expression of α-ENaC, β-ENaC, and γ-ENaC as analyzed by Western blot from plasma membrane proteins. Western blot analysis of the expression of α-ENaC and β-ENaC was performed using native samples. Expression of γ-ENaC was done using peptide:*N*-glycosidase F-treated samples. Blots were additionally stained for total protein content. *E*: color bars representing signal intensity. *F*–*L*: densitometric analysis of Western blot results from two gels and $n = 5$ or 6 per group normalized for the total protein signal of each lane. Values are expressed relative to the average of the healthy control group. *Significant difference compared with control mice. prox., proximal.

DISCUSSION

This study demonstrates the stimulation of proteolytic activation of α-ENaC and γ-ENaC in the mouse kidney under physiological conditions and most importantly in experimental nephrotic syndrome, which was a missing proof in our previous efforts (13, 15, 16, 18). The detection and discrimination of cleavage products of γ-ENaC in Western blot was accomplished using another antibody as previously used and, most importantly, after deglycosylation of the kidney lysate, which was recently reported by Frindt et al. (23) simultaneously with our efforts (6, 31). One possible reason for the improved separation of γ-ENaC cleavage products after deglycosylation might be related to the improved binding of SDS to the protein chain lacking negatively charged *N*-glycosylated residues. This will lead to a more homogenous charge of both cleavage products so that the mass difference of 5 kDa between the products is better resolved during electrophoresis.

In the study of Frindt et al. (23), γ-ENaC expression was investigated in both mice and rats as well as in ENaC-

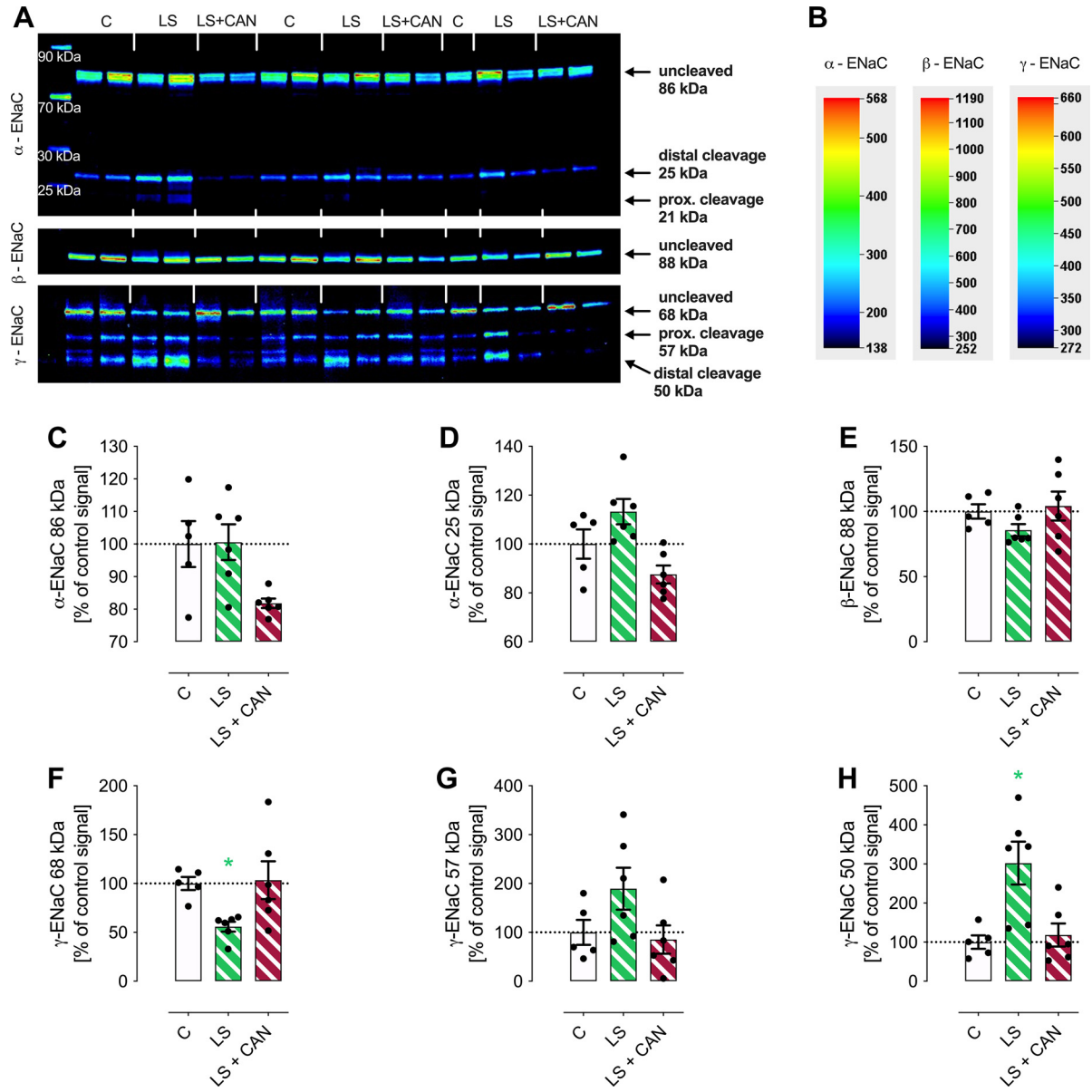

Figure 5. Effect of blockade of the mineralocorticoid receptor on expression of epithelial Na^+ channel (ENaC) subunits in the kidney cortex of mice under a low-salt diet (LS). Mice were treated for 2 days with LS with or without canrenoate (CAN) in the drinking bottle (400 mg/L, corresponding to an intake of ~80 µg/g). *A*: expression of α-ENaC, β-ENaC, and γ-ENaC analyzed by Western blot from plasma membrane proteins. Western blot analysis of the expression of α-ENaC and β-ENaC was performed using native samples. Expression of γ-ENaC was done using peptide:*N*-glycosidase F-treated samples. Blots were additionally stained for total protein content. *B*: color bars representing signal intensity. *C–H*: densitometric analysis of Western blot results normalized for the total protein signal of each lane. Values are expressed relative to the average of the healthy control group (C). *Significant difference compared with control mice. prox., proximal.

expressing FRT cells using a custom-made antibody directed against the same COOH-terminal sequence of γ-ENaC as that of the commercial antibody used in this study. In both rats and FRT cells, the authors found three bands migrating at 65, 55, and 50 kDa, which were interpreted to represent full-length, furin-cleaved, and doubly cleaved γ-ENaC. The observed migration pattern of γ-ENaC in that study was identical to that observed in mouse kidneys of our study. Currently, proteolytic activation of ENaC is thought to occur sequentially by the intracellular serine protease furin cleaving α-ENaC twice and γ-ENaC once, leaving a final proteolytic event at the distal γ-ENaC (4, 8). This concept is mainly derived from heterologous expression systems such as the above-mentioned FRT cells, mouse collecting duct cells (32), or oocytes from *Xenopus laevis* (6), which, however, might be confounded by endogenous serine proteases. Moreover, this concept suggests that proteolytic activation of α-ENaC is almost complete and cannot be increased further. Our data demonstrate that ENaC is proteolytically processed under physiological and nephrotic conditions at both the α- and γ-subunit in vivo. This suggests a complex action of different serine proteases or cascades thereof that must not necessarily involve furin. Therefore, instead of referring to furin-cleaved and doubly cleaved α-ENaC and γ-ENaC, we

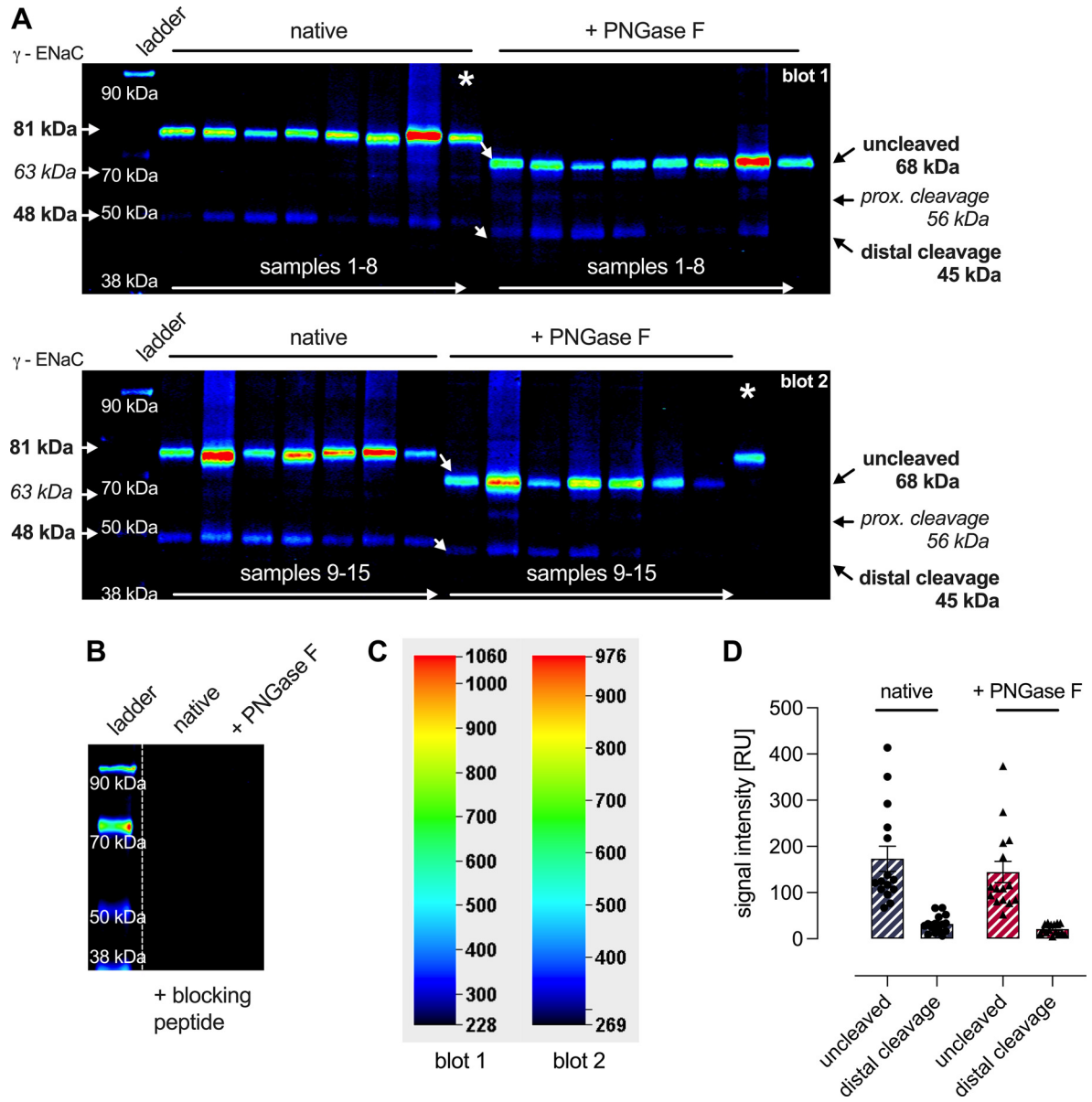

Figure 6. Expression of γ-epithelial Na^+ channel (ENaC) in human nephrectomy specimens and the effect of deglycosylation. *A*: expression of the γ-subunit of ENaC from kidneys of 15 patients undergoing tumor nephrectomy. Western blots from plasma membrane proteins with or without treatment with peptide:*N*-glycosidase F for deglycosylation. Blots were additionally stained for total protein content. The sample marked with the asterisk was used on both blots for normalization. *B*: administration of the blocking peptide for γ-ENaC attenuated all bands. The alignment of the samples was rearranged as indicated by the dashed line. *C*: color bars representing the signal intensity of each blot. *D*: densitometric analysis of the expression of full-length γ-ENaC and its cleavage product (48 kDa resp. 45 kDa) normalized for the total protein signal of each lane. Note that the proximal cleavage product at 63 kDa resp. 56 kDa does not reach a sufficient signal-to-noise ratio and, therefore, was not analyzed with densitometry. prox., proximal.

preferred to refer to these cleavage products as proximally and distally cleaved α-ENaC and γ-ENaC designated from the NH_2-terminus of the subunit, respectively. This allows a neutral view on proteolytic events in both subunits. For α-ENaC using a NH_2-terminal antibody, we noticed two cleavage products at 25 and 21 kDa, the latter of which was almost absent in the healthy state. For γ-ENaC using a COOH-terminal antibody, there were two cleavage products at 57 and 50 kDa. The data are compatible with proteolytic activation by removal of inhibitory tracts from both subunits (Fig. 7). However, the data could also be interpreted that proteolytic activation could also occur by a single distal cleavage at both subunits without complete removal of the inhibitory tract. This notion is particularly suggested by the results obtained with the NH_2-terminal antibody against α-ENaC that might distinguish proximal and distal cleavage. In low-salt-treated or nephrotic mice, we found dominant expression of the larger cleavage product at 25 kDa, which might indicate absence of proximal cleavage that would be indicated by the formation of the 21-kDa fragment. However, without identification of the sequence of these cleavage products, it is impossible to tell whether they truly represent proximal or distal cleavage or if one of them might be a functionally irrelevant cleavage product. For γ-ENaC, the

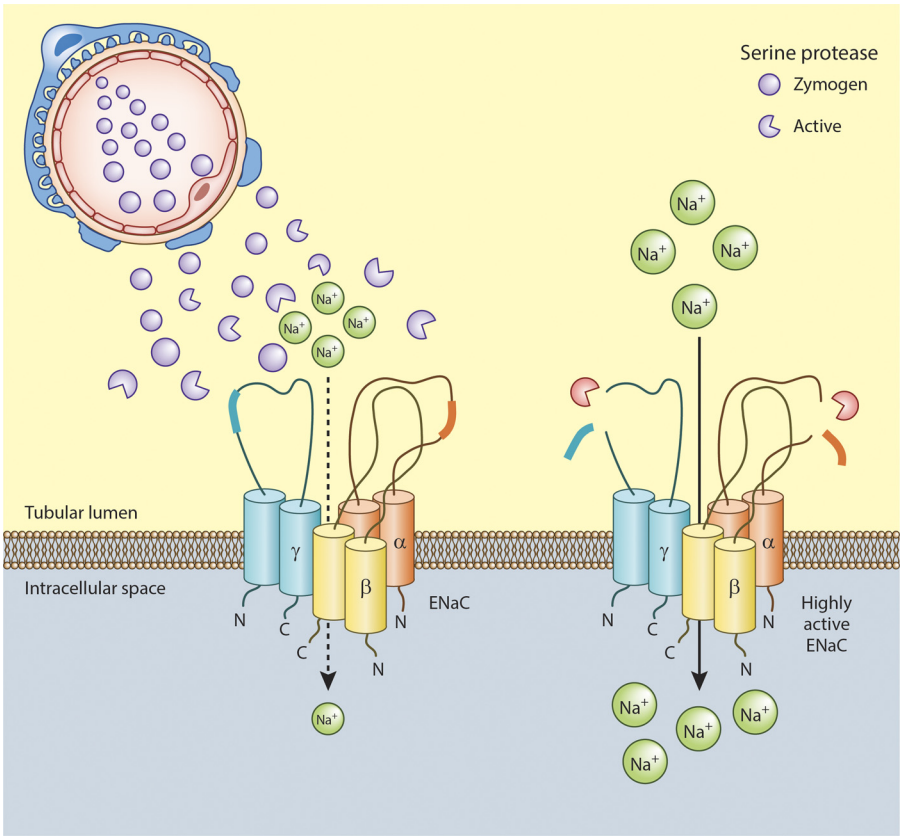

Figure 7. Current model of proteolytic epithelial Na^+ channel (ENaC) activation in experimental nephrotic syndrome. Glomerular proteinuria leads to aberrant filtration of serine proteases, which activate ENaC by cleavage at both the α- and γ-subunit, leading to the removal of inhibitory tracts. However, the cleavage at the distal site of both α-ENaC and, more importantly, γ-ENaC might also be sufficient to maximally stimulate the channel. The identity of the essential serine protease(s) is not known, and there is the possibility that the α- and γ-subunits are cleaved by different serine proteases.

distinction between proximal and distal cleavage is even impossible to delineate using the COOH-terminal antibody, and, unfortunately, NH_2-terminal antibodies or cleavage site-specific antibodies were not available. It is conceivable that a single cleavage event in both distal cleavage sites may be sufficient to activate ENaC, particularly at the γ-subunit, which seems to have a very high impact on channel activation (9). In *Xenopus* oocytes expressing αβγ-ENaC, the addition of serine proteases such as trypsin or chymotrypsin results in a strong increase of channel activity (6, 17, 18, 33). In single-channel recordings, it was found that addition of trypsin increased the number of open channels without an effect on channel expression (33, 34). This finding was explained by the recruitment of near-silent channels that are expressed at the cell surface without previous proteolytic activation and results from a single proteolytic event by an aprotinin-sensitive extracellular protease (34).

The most robust finding of the Western blot analyses shown in Figs. 2–4 was the upregulation of the cleavage products of α-ENaC and γ-ENaC at 25 and 50 kDa, respectively, representing cleavage at the distal cleavage site of both subunits. Remarkably, there was no difference between proteolytic activation in nephrotic mice regardless of the model (doxorubicin or podocin deficiency) and also healthy mice. Up to now, the identity of the membrane-bound or soluble serine proteases that mediate proteolytic activation of ENaC remain unclear, which is particularly true for nephrotic syndrome. A recent study by our group has characterized the abundance of all serine protease in healthy and nephrotic urine using proteomics (35). Whereas in health renally expressed serine proteases such as urokinase-type plasminogen activator (uPA) or prostasin were identified, the most dominant serine protease in nephrotic urine was plasminogen in addition to other proteases from the coagulation and complement system. However, we could demonstrate that mice deficient for uPA or plasminogen still developed Na^+ retention in experimental nephrotic syndrome, indicating that the uPA-plasminogen axis seems not to be essential for proteolytic ENaC activation in nephrotic mouse models (15, 16, 36, 37). Noteworthy, aprotinin was similarly effective in nephrotic plasminogen-deficient mice (15). Another study identified the cysteine protease cathepsin B in the urine of podocin-deficient nephrotic mice that stimulated amiloride-sensitive currents in collecting duct cells (38). Further efforts are required to identify the relevant serine proteases in both health and nephrotic syndrome.

We confirmed the stimulation of cleavage of γ-ENaC by a low-salt diet as previously reported by Frindt et al. (23). In addition, we found increased cleavage at the α-subunit. Furthermore, our data with canrenoate demonstrate that ENaC cleavage under a low-salt diet is mediated by aldosterone (Fig. 5). Currently, it is unclear how aldosterone exerts this MR-dependent effect and which proteases are involved. Candidates include membrane-bound serine proteases such as matriptase or prostasin. We previously reported that the scaffold function of prostasin is necessary for full proteolytic ENaC activation of the γ-subunit in healthy mice under ENaC blockade with triamterene (6). However, enzymatic activity of prostasin was not essential and prostasin expression was not increased despite excessive hyperaldosteronism in

these mice, pointing to another serine protease responsible for proteolytic ENaC processing. In this study and the previous study by Essigke et al. (6), ENaC blockade by triamterene has proven to be a strong stimulus of proteolytic ENaC activation. This could be related not only to the increased plasma aldosterone concentration detected soon after ENaC blockade (16) but also to the effects of reduced intracellular Na^+ concentration, which is a strong stimulus of maturation and proteolytic ENaC processing in cultured cells (39). Along the lines, a low-Na^+ diet could also induce proteolytic ENaC activation by reducing intracellular Na^+ concentration.

In contrast to the findings in healthy mice, MR blockade did not prevent proteolytic ENaC activation in nephrotic mice despite hyperaldosteronism, which is consistent with the notion that aberrantly filtered serine proteases are responsible for proteolytic ENaC activation in experimental nephrotic syndrome (Fig. 2). Accordingly, treatment of nephrotic mice with aprotinin prevented the formation of ENaC cleavage products and Na^+ retention. It is also remarkable that proteolytic ENaC activation is prevented by aprotinin in nephrotic mice but not in healthy mice (31), suggesting a different mechanism of proteolytic ENaC activation in healthy versus nephrotic mice, possibly related to membrane-bound proteases versus soluble proteases. Despite the strong evidence in favor of proteolytic ENaC activation by proteasuria, a possible role of hyperaldosteronism in Na^+ retention cannot be denied completely as hyperaldosteronism is expected to exert independent effects on ENaC expression and proteolytic activation. According to an integrative concept proposed by our group, overfill caused by proteasuria and underfill indicated by hyperaldosteronism are not mutually exclusive and might coexist, for example, in murine doxorubicin-induced nephrotic syndrome or minimal change disease in children (11). As a consequence, both factors will act synergistically to stimulate ENaC activation and Na^+ retention.

In human nephrectomy samples, a very similar migration pattern of γ-ENaC and its cleavage products could be obtained as in mice. The shift of full-length γ-ENaC on deglycosylation was 13 kDa and was in agreement with the value reported by Zachar et al. (40), who demonstrated a shift of 13–15 kDa. Interestingly, distally cleaved γ-ENaC at 48 kDa was detectable in native samples without deglycosylation, and the expression was much higher than that of proximally cleaved γ-ENaC at 63 kDa, which was barely detectable. These findings are consistent with the existence of proteolytic activation of γ-ENaC in humans, which was also suggested by an immunohistochemical study using an antibody against distally cleaved γ-ENaC (41). In that study, this cleavage product migrated between 42 and 45 kDa, which is in good agreement with the values obtained in this study. Unfortunately, we were not able to demonstrate proteolytic activation of ENaC in human nephrotic syndrome due to the lack of tissue from such patients.

A limitation of the present study might be the analysis of whole cell kidney lysates, which cannot distinguish between intracellularly and extracellularly expressed ENaC. To isolate cell surface-expressed ENaC, Frindt, Palmer, and colleagues developed an in vivo biotinylation method that has been successfully implemented in rats and mice (27, 42, 43). However, we think that our results regarding the expression of distally cleaved γ-ENaC reflects channel activation in vivo as the final proteolysis of γ-ENaC is thought to take place in the extracellular space on the cell surface. Even after internalization, distally cleaved γ-ENaC can be recycled to the cell surface (44). Therefore, the increased expression of distally cleaved γ-ENaC clearly points to stimulated Na^+ transport, which could be induced by dietary and pharmacological maneuvers as well as by the induction of proteasuria during nephrotic syndrome. It is remarkable that the cleavage product of γ-ENaC at 50 kDa indicating distal cleavage by an extracellular serine protease behaved as a biomarker paralleling renal Na^+ avidity. The modulation of the expression of this cleavage product also indicates that in the mouse kidney not all γ-ENaC subunits are cleaved and that there is a channel subpopulation that can be proteolytically activated. Noteworthy, concomitant proteolytic activation of α-ENaC indicated by the expression of the 25-kDa band was also prominent in these conditions.

Perspectives and Significance

This study presents the missing link between experimental nephrotic syndrome and proteolytic activation of ENaC in vivo. Inhibition of proteolytic ENaC activation could emerge as a new therapeutic approach in nephrotic syndrome.

GRANTS

This work was supported by Deutsche Forschungsgemeinschaft Grant AR 1092/2-2 (to F.A.).

DISCLOSURES

No conflicts of interest, financial or otherwise, are declared by the authors.

AUTHOR CONTRIBUTIONS

B.N.B. and F.A. conceived and designed research; B.N.B., D.E., A.J., J.C.S., M.W., M.Z.K., M.X., L.K., K.O., J.H., and B.A. performed experiments; B.N.B., D.E., A.J., J.C.S., M.W., and F.A. analyzed data; B.N.B. and F.A. interpreted results of experiments; B.N.B. prepared figures; F.A. drafted manuscript; B.N.B., D.E., A.L.B., and F.A. edited and revised manuscript; F.A. approved final version of manuscript.

REFERENCES

1. **Rossier BC**, **Stutts MJ.** Activation of the epithelial sodium channel (ENaC) by serine proteases. *Annu Rev Physiol* 71: 361–379, 2009. doi:10.1146/annurev.physiol.010908.163108.
2. **Kleyman TR**, **Eaton DC.** Regulating ENaC's gate. *Am J Physiol Cell Physiol* 318: C150–C162, 2020. doi:10.1152/ajpcell.00418.2019.
3. **Carattino MD**, **Sheng S**, **Bruns JB**, **Pilewski JM**, **Hughey RP**, **Kleyman TR.** The epithelial Na^+ channel is inhibited by a peptide derived from proteolytic processing of its alpha subunit. *J Biol Chem* 281: 18901–18907, 2006. doi:10.1074/jbc.M604109200.
4. **Hughey RP**, **Bruns JB**, **Kinlough CL**, **Harkleroad KL**, **Tong Q**, **Carattino MD**, **Johnson JP**, **Stockand JD**, **Kleyman TR.** Epithelial sodium channels are activated by furin-dependent proteolysis. *J Biol Chem* 279: 18111–18114, 2004. doi:10.1074/jbc.C400080200.
5. **Bruns JB**, **Carattino MD**, **Sheng S**, **Maarouf AB**, **Weisz OA**, **Pilewski JM**, **Hughey RP**, **Kleyman TR.** Epithelial Na^+ channels are fully activated by furin- and prostasin-dependent release of an inhibitory

peptide from the gamma-subunit. *J Biol Chem* 282: 6153–6160, 2007. doi:10.1074/jbc.M610636200.

6. **Essigke D**, **Ilyaskin AV**, **Wörn M**, **Bohnert BN**, **Xiao M**, **Daniel C**, **Amann K**, **Birkenfeld AL**, **Szabo R**, **Bugge TH**, **Korbmacher C**, **Artunc F.** Zymogen-locked mutant prostasin (Prss8) leads to incomplete proteolytic activation of the epithelial sodium channel (ENaC) and severely compromises triamterene tolerance in mice. *Acta Physiol (Oxf)* 232: e13640, 2021. doi:10.1111/apha.13640.
7. **Patel AB**, **Chao J**, **Palmer LG.** Tissue kallikrein activation of the epithelial Na channel. *Am J Physiol Renal Physiol* 303: F540–F550, 2012. doi:10.1152/ajprenal.00133.2012.
8. **Passero CJ**, **Hughey RP**, **Kleyman TR.** New role for plasmin in sodium homeostasis. *Curr Opin Nephrol Hypertens* 19: 13–19, 2010. doi:10.1097/MNH.0b013e3283330fb2.
9. **Carattino MD**, **Hughey RP**, **Kleyman TR.** Proteolytic processing of the epithelial sodium channel gamma subunit has a dominant role in channel activation. *J Biol Chem* 283: 25290–25295, 2008. doi:10.1074/jbc.M803931200.
10. **Artunc F.** Proteolytic activation of the epithelial sodium channel in nephrotic syndrome by proteasuria: concept and therapeutic potential. *Turk J Nephrol* 29: 59–65, 2020. doi:10.5152/turkjnephrol.2020.4227.
11. **Artunc F**, **Wörn M**, **Schork A**, **Bohnert BN.** Proteasuria-the impact of active urinary proteases on sodium retention in nephrotic syndrome. *Acta Physiol (Oxf)* 225: e13249, 2019. doi:10.1111/apha.13249.
12. **Hinrichs GR**, **Jensen BL**, **Svenningsen P.** Mechanisms of sodium retention in nephrotic syndrome. *Curr Opin Nephrol Hypertens* 29: 207–212, 2020. doi:10.1097/MNH.0000000000000578.
13. **Bohnert BN**, **Menacher M**, **Janessa A**, **Wörn M**, **Schork A**, **Daiminger S**, **Kalbacher H**, **Häring HU**, **Daniel C**, **Amann K**, **Sure F**, **Bertog M**, **Haerteis S**, **Korbmacher C**, **Artunc F.** Aprotinin prevents proteolytic epithelial sodium channel (ENaC) activation and volume retention in nephrotic syndrome. *Kidney Int* 93: 159–172, 2018. doi:10.1016/j.kint.2017.07.023.
14. **Dizin E**, **Olivier V**, **Maire C**, **Komarynets O**, **Sassi A**, **Roth I**, **Loffing J**, **de Seigneux S**, **Maillard M**, **Rutkowski JM**, **Edwards A**, **Feraille E.** Time-course of sodium transport along the nephron in nephrotic syndrome: the role of potassium. *FASEB J* 34: 2408–2424, 2020. doi:10.1096/fj.201901345R.
15. **Xiao M**, **Bohnert BN**, **Aypek H**, **Kretz O**, **Grahammer F**, **Aukschun U**, **Wörn M**, **Janessa A**, **Essigke D**, **Daniel C**, **Amann K**, **Huber TB**, **Plow EF**, **Birkenfeld AL**, **Artunc F.** Plasminogen deficiency does not prevent sodium retention in a genetic mouse model of experimental nephrotic syndrome. *Acta Physiol (Oxf)* 231: e13512, 2021. doi:10.1111/apha.13512.
16. **Bohnert BN**, **Daiminger S**, **Wörn M**, **Sure F**, **Staudner T**, **Ilyaskin AV**, **Batbouta F**, **Janessa A**, **Schneider JC**, **Essigke D**, **Kanse S**, **Haerteis S**, **Korbmacher C**, **Artunc F.** Urokinase-type plasminogen activator (uPA) is not essential for epithelial sodium channel (ENaC)-mediated sodium retention in experimental nephrotic syndrome. *Acta Physiol (Oxf)* 227: e13286, 2019. doi:10.1111/apha.13286.
17. **Haerteis S**, **Krappitz M**, **Diakov A**, **Krappitz A**, **Rauh R**, **Korbmacher C.** Plasmin and chymotrypsin have distinct preferences for channel activating cleavage sites in the γ subunit of the human epithelial sodium channel. *J Gen Physiol* 140: 375–389, 2012. doi:10.1085/jgp.201110763.
18. **Haerteis S**, **Schork A**, **Dörffel T**, **Bohnert BN**, **Nacken R**, **Wörn M**, **Xiao M**, **Essigke D**, **Janessa A**, **Schmaier AH**, **Feener EP**, **Häring HU**, **Bertog M**, **Korbmacher C**, **Artunc F.** Plasma kallikrein activates the epithelial sodium channel in vitro but is not essential for volume retention in nephrotic mice. *Acta Physiol (Oxf)* 224: e13060, 2018. doi:10.1111/apha.13060.
19. **Canessa CM**, **Merillat AM**, **Rossier BC.** Membrane topology of the epithelial sodium channel in intact cells. *Am J Physiol Cell Physiol* 267: C1682–C1690, 1994. doi:10.1152/ajpcell.1994.267.6.C1682.
20. **Kashlan OB**, **Kinlough CL**, **Myerburg MM**, **Shi S**, **Chen J**, **Blobner BM**, **Buck TM**, **Brodsky JL**, **Hughey RP**, **Kleyman TR.** N-linked glycans are required on epithelial Na^+ channel subunits for maturation and surface expression. *Am J Physiol Renal Physiol* 314: F483–F492, 2018. doi:10.1152/ajprenal.00195.2017.
21. **Hughey RP**, **Mueller GM**, **Bruns JB**, **Kinlough CL**, **Poland PA**, **Harkleroad KL**, **Carattino MD**, **Kleyman TR.** Maturation of the epithelial Na^+ channel involves proteolytic processing of the alpha- and gamma-subunits. *J Biol Chem* 278: 37073–37082, 2003. doi:10.1074/jbc.M307003200.
22. **Ergonul Z**, **Frindt G**, **Palmer LG.** Regulation of maturation and processing of ENaC subunits in the rat kidney. *Am J Physiol Renal Physiol* 291: F683–F693, 2006. doi:10.1152/ajprenal.00422.2005.
23. **Frindt G**, **Shi S**, **Kleyman TR**, **Palmer LG.** Cleavage state of γENaC in mouse and rat kidneys. *Am J Physiol Renal Physiol* 320: F485–F491, 2021. doi:10.1152/ajprenal.00536.2020.
24. **Artunc F**, **Nasir O**, **Amann K**, **Boini KM**, **Häring HU**, **Risler T**, **Lang F.** Serum- and glucocorticoid-inducible kinase 1 in doxorubicin-induced nephrotic syndrome. *Am J Physiol Renal Physiol* 295: F1624–F1634, 2008. doi:10.1152/ajprenal.00032.2008.
25. **Bohnert BN**, **Daniel C**, **Amann K**, **Voelkl J**, **Alesutan I**, **Lang F**, **Heyne N**, **Häring HU**, **Artunc F.** Impact of phosphorus restriction and vitamin D-substitution on secondary hyperparathyroidism in a proteinuric mouse model. *Kidney Blood Press Res* 40: 153–165, 2015. doi:10.1159/000368491.
26. **Bohnert BN**, **Artunc F.** Induction of nephrotic syndrome in mice by retrobulbar injection of doxorubicin and prevention of volume retention by sustained release aprotinin. *J Vis Exp* 2018: 57642, 2018. doi:10.3791/57642.
27. **Yang L**, **Frindt G**, **Lang F**, **Kuhl D**, **Vallon V**, **Palmer LG.** SGK1-dependent ENaC processing and trafficking in mice with high dietary K intake and elevated aldosterone. *Am J Physiol Renal Physiol* 312: F65–F76, 2017. doi:10.1152/ajprenal.00257.2016.
28. **Masilamani S**, **Kim GH**, **Mitchell C**, **Wade JB**, **Knepper MA.** Aldosterone-mediated regulation of ENaC alpha, beta, and gamma subunit proteins in rat kidney. *J Clin Invest* 104: R19–R23, 1999. doi:10.1172/JCI7840.
29. **Deschenes G**, **Doucet A.** Collecting duct (Na^+-K^+)-ATPase activity is correlated with urinary sodium excretion in rat nephrotic syndromes. *J Am Soc Nephrol* 11: 604–615, 2000. doi:10.1681/ASN.V114604.
30. **Frindt G**, **Yang L**, **Bamberg K**, **Palmer LG.** Na restriction activates epithelial Na channels in rat kidney through two mechanisms and decreases distal Na^+ delivery. *J Physiol* 596: 3585–3602, 2018. doi:10.1113/JP275988.
31. **Wörner S**, **Bohnert BN**, **Wörn M**, **Xiao M**, **Janessa A**, **Birkenfeld AL**, **Amann K**, **Daniel C**, **Artunc F.** Renal effects of the serine protease inhibitor aprotinin in healthy conscious mice. *Acta Pharmacol Sin*. 2021 Mar 23. doi:10.1038/s41401-021-00628-1. Epub ahead of print.
32. **Nesterov V**, **Dahlmann A**, **Bertog M**, **Korbmacher C.** Trypsin can activate the epithelial sodium channel (ENaC) in microdissected mouse distal nephron. *Am J Physiol Renal Physiol* 295: F1052–F1062, 2008. doi:10.1152/ajprenal.00031.2008.
33. **Diakov A**, **Bera K**, **Mokrushina M**, **Krueger B**, **Korbmacher C.** Cleavage in the γ-subunit of the epithelial sodium channel (ENaC) plays an important role in the proteolytic activation of near-silent channels. *J Physiol* 586: 4587–4608, 2008. doi:10.1113/jphysiol.2008.154435.
34. **Caldwell RA**, **Boucher RC**, **Stutts MJ.** Serine protease activation of near-silent epithelial Na^+ channels. *Am J Physiol Cell Physiol* 286: C190–C194, 2004. doi:10.1152/ajpcell.00342.2003.
35. **Wörn M**, **Bohnert BN**, **Alenazi F**, **Boldt K**, **Klose F**, **Junger K**, **Ueffing M**, **Birkenfeld AL**, **Kalbacher H**, **Artunc F.** Proteasuria in nephrotic syndrome-quantification and proteomic profiling. *J Proteomics* 230: 103981, 2021. doi:10.1016/j.jprot.2020.103981.
36. **Hinrichs GR**, **Weyer K**, **Friis UG**, **Svenningsen P**, **Lund IK**, **Nielsen R**, **Mollet G**, **Antignac C**, **Bistrup C**, **Jensen BL**, **Birn H.** Urokinase-type plasminogen activator contributes to amiloride-sensitive sodium retention in nephrotic range glomerular proteinuria in mice. *Acta Physiol (Oxf)* 227: e13362, 2019. doi:10.1111/apha.13362.
37. **Bohnert BN**, **Kanse S**, **Haerteis S**, **Korbmacher C**, **Artunc F.** Rebuttal to editorial: Sodium retention by uPA in nephrotic syndrome? *Acta Physiol (Oxf)* 228: e13427, 2020. doi:10.1111/apha.13427.
38. **Larionov A**, **Dahlke E**, **Kunke M**, **Zanon Rodriguez L**, **Schiessl IM**, **Magnin JL**, **Kern U**, **Alli AA**, **Mollet G**, **Schilling O**, **Castrop H**, **Theilig F.** Cathepsin B increases ENaC activity leading to hypertension early in nephrotic syndrome. *J Cell Mol Med* 23: 6543–6553, 2019. doi:10.1111/jcmm.14387.
39. **Heidrich E**, **Carattino MD**, **Hughey RP**, **Pilewski JM**, **Kleyman TR**, **Myerburg MM.** Intracellular Na^+ regulates epithelial Na^+ channel

maturation. *J Biol Chem* 290: 11569–11577, 2015. doi:10.1074/jbc.M115.640763.

40. **Zachar R**, **Mikkelsen MK**, **Skjødt K**, **Marcussen N**, **Zamani R**, **Jensen BL**, **Svenningsen P.** The epithelial Na^+ channel α- and γ-subunits are cleaved at predicted furin-cleavage sites, glycosylated and membrane associated in human kidney. *Pflugers Arch* 471: 1383–1396, 2019. doi:10.1007/s00424-019-02321-z.
41. **Zachar RM**, **Skjødt K**, **Marcussen N**, **Walter S**, **Toft A**, **Nielsen MR**, **Jensen BL**, **Svenningsen P.** The epithelial sodium channel γ-subunit is processed proteolytically in human kidney. *J Am Soc Nephrol* 26: 95–106, 2015. doi:10.1681/ASN.2013111173.
42. **Frindt G**, **Ergonul Z**, **Palmer LG.** Surface expression of epithelial Na channel protein in rat kidney. *J Gen Physiol* 131: 617–627, 2008. doi:10.1085/jgp.200809989.
43. **Patel AB**, **Frindt G**, **Palmer LG.** Feedback inhibition of ENaC during acute sodium loading in vivo. *Am J Physiol Renal Physiol* 304: F222–F232, 2013. doi:10.1152/ajprenal.00596.2012.
44. **Frindt G**, **Gravotta D**, **Palmer LG.** Regulation of ENaC trafficking in rat kidney. *J Gen Physiol* 147: 217–227, 2016. doi:10.1085/jgp.201511533.